

# Chapter 1

## Liutex and Third Generation of Vortex Definition and Identification



Chaoqun Liu, Habib Ahmari, Charles Nottage, Yifei Yu, Oscar Alvarez, and Vishwa Patel

**Abstract** Liutex is a physical quantity like velocity, vorticity, pressure, temperature, etc., describing local fluid rotation or vortex, which was ignored for centuries. Liutex was defined by the University of Arlington at Texas (UTA) team in 2018 as a vector for vortex. Its direction is the local rotation axis, and magnitude is twice local angular rotation speed. As the third generation of vortex definition and identification, Liutex has been widely applied for visualization of vortex structure to replace the first generation or vorticity, which cannot distinguish shear from rotation and the second generation such as  $Q$ ,  $\Delta$ ,  $\lambda_2$ , and  $\lambda_{ci}$  methods, which are all scalar without rotation axis, dependent on threshold and contaminated by shear and stretching. Several new vortex identification methods have been developed, especially the modified Liutex-Omega method, which is threshold insensitive, and the Liutex-Core-Line method, which is unique and threshold-free. According to the Liutex vector, a unique coordinate system called Principal Coordinate can be set up, and consequent Principal Decomposition of velocity gradient tensor can be made. Different from classical fluid kinematics, the Liutex-based new fluid kinematics decomposes the fluid motion to a rotational part and a non-rotational part (*UTA R-NR* decomposition). The non-rotational part can be further decomposed to stretching and shear consisting of symmetric shear and anti-symmetric shear in contrast with the classical fluid kinematics, which decomposes fluid motion to deformation and vorticity, that was misunderstood as rotation. According to the constitutive relation between stress and strain, the new fluid kinematics may give significant influence to new fluid dynamics.

### 1.1 Introduction

A vortex is intuitively recognized as a rotational/swirling motion of fluids. It is ubiquitous in nature and viewed as the building blocks, muscles, and sinews of turbulent flows [1]. Quantitative understanding of vortex is essential for turbulence research

---

C. Liu (✉) · H. Ahmari · C. Nottage · Y. Yu · O. Alvarez · V. Patel  
University of Texas at Arlington, Arlington, TX, USA  
e-mail: [cliu@uta.edu](mailto:cliu@uta.edu)

and many engineering applications such as hydrodynamics, aerodynamics, thermodynamics, oceanography, meteorology, metallurgy, civil engineering, astronomy, biology, etc. In 1858, Helmholtz first defined vortex as tubes composed of so-called vortex filaments [2], which are, in fact, infinitesimal vorticity tubes. Vorticity has a rigorous mathematical definition with no clear physical meaning.

Conversely, vortex has a physical meaning but no mathematical definition until recently. Science and engineering applications have shown that the correlation between vortex and vorticity is very weak, especially in the near-wall region [3]. Also, existing vortex identification methods, which are based on eigenvalues of the velocity gradient tensor, are scalars and therefore strongly depend on the arbitrary thresholds.

*Liutex* is a new physical quantity introduced by Liu et al. in 2018 [4–6] that represents local fluid rotation, i.e., vortex, and is a mathematically rigorous tool for vortex characterization. The major idea of *Liutex* is to extract the rigid rotation part from the fluid motion to represent the vortex. Given the novelty of *Liutex*, it is inevitable that the vortex dynamics be re-examined to develop unique and accurate vortex identification methods independent of thresholds. This chapter presents the existing vortex definition and identification methods and their limitations, and introduces *Liutex*, as the third generation of vortex definition, and *Liutex*-based vortex Identification methods.

## 1.2 Three Generations of Vortex Definition and Identification

There are three generations of vortex identification methods [6], and Helmholtz's [2] definition of vortex is classified as the first. During the past four decades, several vortex identification criteria, such as  $Q$ ,  $\Delta$ ,  $\lambda_2$ , and  $\lambda_{ci}$  methods, have been developed [7–11] and are classified as the second generation of vortex identification. They are all based on eigenvalues of the velocity gradient tensor; however, they are scalars and thus strongly dependent on the arbitrary thresholds when plotting the iso surface to represent vortical structures. They cannot show the vortex rotation axis, which is critical for vortex structure. Furthermore, they are all contaminated by stretching (compression) and shearing. Rotational axis and uniqueness in strength are two important issues for vortex definition that cannot be solved by either the first or second vortex identification methods.

*Liutex*, the third generation of vortex definition and identification, was introduced by the first author Dr. Liu at the University of Texas at Arlington (UTA) [4–6]. It is defined as a vector that uses the real eigenvector of velocity gradient tensor as its direction and twice the local angular speed of the rigid rotation as its magnitude. The major idea of *Liutex* is to extract the rigid rotation part from fluid motion to represent vortex, which is a mathematically rigorous tool suitable for vortex characterization [12]. The location of the rotation axis is then the local maxima of *Liutex*

(not vorticity), and the Liutex magnitude is twice the vortex angular speed, which is uniquely defined. Although similar ideas of decomposition of vorticity tensor to a pure rotation and anti-symmetric shear have been given by [13, 14], they did not find a vector definition for flow rotation or Liutex. Several vortex identification methods have been developed based on the Liutex definition [4–6, 15–39]. Examples of these methods are modified *Liutex-Omega* and *Liutex-Core-Line*. The former is threshold insensitive, and the latter is threshold-free. These methods have been shown to accurately visualize vortical structures in turbulent flows [40, 41]; however, schemes and software for automated generation and case-independent features are still open for research. The current methods still have parameters that need manual adjusting.

### 1.2.1 *First Generation of Vortex Identification Methods (Vorticity-Based Methods)*

Since Helmholtz proposed the concepts of vorticity tube and filament in 1858 [2], it has generally been believed that vortices consist of vorticity tubes, and vortex strength is measured by the magnitude of vorticity, i.e.,  $\nabla \times \vec{v}$  [42]. Although vorticity is widely adopted for detecting vortices, one immediate counterexample is that the average shear force generated by the no-slip wall in the laminar boundary layer is so strong that a very large amount of vorticity exists. However, no rotation motions are observed in the near-wall regions. This implies that vortex cannot be represented by vorticity. Robinson [43] found that “the association between regions of strong vorticity and actual vortices can be rather weak in the turbulent boundary layer, especially in the near-wall region.” In 1990, Wang et al. [30] showed that the magnitude of vorticity could be substantially reduced along vorticity lines by entering the vortex core region near the solid wall in a flat plate boundary layer. Figure 1.1 clearly indicates that for a transitional flow over a flat plate in the near-wall region of the boundary layer, the local vorticity vector can deviate from the direction of vortical structures. Also, a vortex can appear in the region where the vorticity is smaller than the surrounding area in which the vorticity is larger than the vorticity inside the vortex. These results demonstrate that vorticity cannot be used to represent vortices, especially in the near-wall region of the boundary layers.

Vortex and vorticity are two different concepts. Vortex is a natural phenomenon, but vorticity is a mathematical definition. In fact, if a vortex cannot be ended inside the flow field, how can turbulence be generated by “vortex breakdown?” Vortex can break down, which means it is not vorticity tube. Although both vortex and vorticity are vectors, they are different vectors.

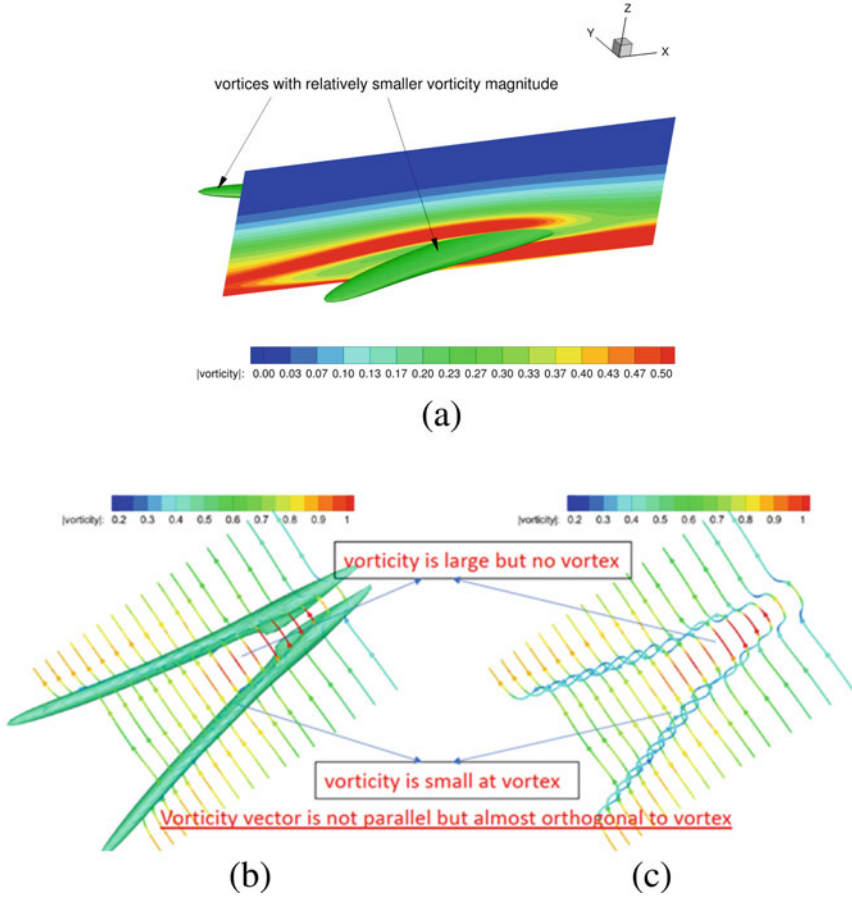


**Fig. 1.1** (a) Vortex appears in the area where vorticity is relatively smaller, (b) vorticity line is not aligned with vortex, (c) vorticity is smaller (green) than surrounding (yellow or red)

### 1.2.2 Second Generation of Vortex Identification

Several vortex identification methods have been proposed during the past four decades, including the  $Q$ ,  $\lambda_{ci}$ , and  $\lambda_2$  methods. These methods are briefly explained in the following.

**$Q$  Method.** The  $Q$  criterion is expressed by Eq. 1.1:

$$Q = \frac{1}{2} (\|\mathbf{B}\|_F^2 - \|\mathbf{A}\|_F^2) \quad (1.1)$$

where  $\mathbf{A}$  and  $\mathbf{B}$  are the symmetric and antisymmetric parts of the velocity gradient tensor, respectively, and  $\|\cdot\|_F^2$  represents the Frobenius norm. Theoretically,  $Q > 0$

can identify the vortex boundary, but in practice, a threshold  $Q_{threshold}$  must be specified to define the regions where  $Q > Q_{threshold}$ .  $Q$ -criterion shows the symmetric tensor roles that balance the anti-symmetric tensor.

**$\lambda_{ci}$  Method.** The  $\lambda_{ci}$  method defines the strength of vortex as the imaginary part  $\lambda_{ci}$  of the complex eigenvalue of the velocity gradient tensor  $\nabla \mathbf{V}$  [10].

**$\lambda_2$  Method.** The  $\lambda_2$  method defines the strength of vortex by using the second negatively largest eigenvalue  $\lambda_2$  of  $A^2 + B^2$ , where  $A$  and  $B$  are the symmetric and anti-symmetric parts of the velocity gradient tensor [9]. Assuming the fluid is incompressible, steady, and non-viscous, the Navier–Stokes equation is converted to  $A^2 + B^2 = -\nabla(p)/\rho$ , where  $p$  and  $\rho$  represent pressure and density, respectively. The rotational area is defined by the existence of two negative eigenvalues of the symmetric tensor  $A^2 + B^2$  [9].

### 1.2.3 Limitations of Existing Vortex Identification Methods

**Thresholds.** Without exception, the abovementioned vortex identification methods require user-specified thresholds. Since different thresholds indicate different vortical structures, it is critical to determine an appropriate threshold. When a large threshold for  $Q$  criterion is used, *vortex breakdown* occurs in the late boundary layer transition (Fig. 1.2a); however, when a small threshold is applied, no *vortex breakdown* occurs (Fig. 1.2b), which means that an appropriate threshold is vital to these vortex identification methods. Many computational results have revealed that the threshold is case-related, empirical, sensitive, time step-related, and hard to adjust. Furthermore, it is unclear whether the specified threshold is proper or improper. There may be no single proper threshold, especially if strong and weak vortices co-exist. If the threshold is too small, weak vortices may be captured, but strong vortices could be smeared and become vague. If the threshold is too large, weak vortices will be wiped out.

**Direction of Rotation.** The other limitation of these vortex identification methods is that they can only provide iso-surface; no information is given about the rotation axis or vortex direction.

**Strength of Vortex.** A more serious question is whether the iso-surface represents the rotation strength. The answer is that they do not, because they are different from each other, though not unique; are contaminated by shear and stretching in different degrees and fail to represent the rigid rotation strength of fluid motion.

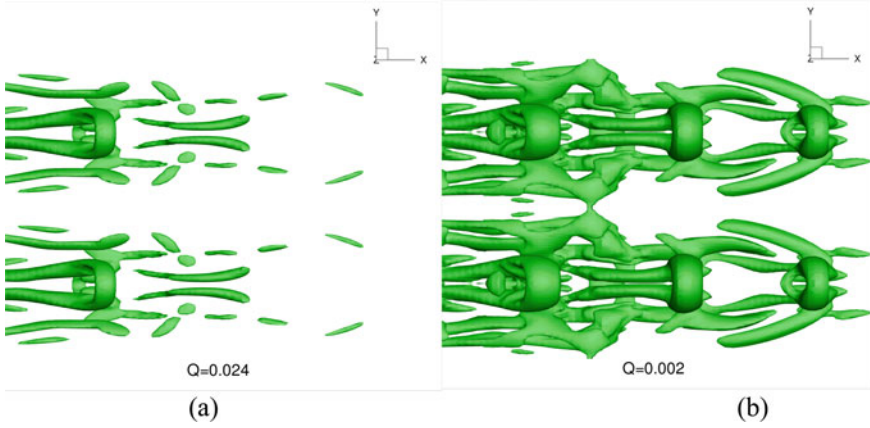


**Fig. 1.2** Vortex breakdown with a large threshold of  $Q = 0.024$  and no vortex breakdown with a small threshold of  $Q = 0.002$  (same DNS dataset)

### 1.2.4 *Mathematical Misunderstandings of the First and Second Generation of Vortex Identification Methods*

The classical theory considers the vorticity vector as the rotation axis and vorticity magnitude as the strength of the vortex (angular speed) [42]. This is correct for solids but not for fluids. It can be shown mathematically that *vorticity is not a fluid rotation axis*, and the first and second generation of vortex identification methods ( $Q$ ,  $\lambda_{ci}$ , and  $\lambda_2$ ) cannot be used as the fluid rotation strength. These methods are contaminated by shear and have different dimensions from the fluid angular speed.

### 1.2.5 *Contaminations of First and Second Generations of Vortex Identification Methods*

**Contamination of Vorticity.** In a principal coordinate, vorticity  $\omega$  and its magnitude  $\|\omega\|$  can be expressed by Eqs. 1.2 and 1.3, respectively:

$$\omega = (\eta, -\xi, R + \epsilon)^T \quad (1.2)$$

$$\|\omega\| = \sqrt{\eta^2 + \xi^2 + (R + \epsilon)^2} \quad (1.3)$$

From Eqs. 1.2 and 1.3, it can be concluded that a vorticity vector not only includes rotation but also claims shear as part of the vortical structure. Here,  $\xi$ ,  $\eta$ ,  $\epsilon$  are all shears but not rotations.

**Contamination of  $Q$  Method.** In a principal coordinate, the velocity gradient tensor  $\nabla \vec{V}$  and  $Q$  value can be written as Eqs. 1.4 and 1.5:

$$\nabla \vec{V} = \begin{bmatrix} \lambda_{cr} & -\frac{1}{2}R & 0 \\ \frac{1}{2}R + \epsilon & \lambda_{cr} & 0 \\ \xi & \eta & \lambda_r \end{bmatrix} = \begin{bmatrix} \lambda_{cr} & \frac{1}{2}\epsilon & \frac{1}{2}\xi \\ \frac{1}{2}\epsilon & \lambda_{cr} & \frac{1}{2}\eta \\ \frac{1}{2}\xi & \frac{1}{2}\eta & \lambda_r \end{bmatrix} + \begin{bmatrix} 0 & -\frac{1}{2}R - \frac{1}{2}\epsilon & -\frac{1}{2}\xi \\ \frac{1}{2}R + \frac{1}{2}\epsilon & 0 & -\frac{1}{2}\eta \\ \frac{1}{2}\xi & \frac{1}{2}\eta & 0 \end{bmatrix} = \mathbf{A}_Q + \mathbf{B}_Q \quad (1.4)$$

$$\begin{aligned} Q &= \frac{1}{2} \left( \|\mathbf{B}_Q\|_F^2 - \|\mathbf{A}_Q\|_F^2 \right) = \frac{1}{2} \left[ 2 \left( \frac{R}{2} + \frac{\epsilon}{2} \right)^2 + 2 \left( \frac{\xi}{2} \right)^2 + 2 \left( \frac{\eta}{2} \right)^2 \right] \\ &\quad - \frac{1}{2} \left[ 2\lambda_{cr}^2 + \lambda_r^2 + 2 \left( \frac{\epsilon}{2} \right)^2 + 2 \left( \frac{\xi}{2} \right)^2 + 2 \left( \frac{\eta}{2} \right)^2 \right] \\ &= \left( \frac{R}{2} \right)^2 + \frac{1}{2} R \cdot \epsilon - \lambda_{cr}^2 - \frac{1}{2} \lambda_r^2 \end{aligned} \quad (1.5)$$

Therefore, the value of  $Q$  is contaminated by shear and stretching. In addition,  $Q$  contains the term of square of  $(R/2)$  indicating dimensional inconsistency with fluid rotation, as  $R/2$  is the angular speed.

**Contamination of  $\lambda_{ci}$  Method.** In a principal coordinate, we have:

$$\frac{R}{2} \left( \frac{R}{2} + \epsilon \right) = \lambda_{ci}^2 \quad (1.6)$$

thus,

$$\lambda_{ci} = \sqrt{\frac{R}{2} \left( \frac{R}{2} + \epsilon \right)} \quad (1.7)$$

The expression of  $\lambda_{ci}$  includes  $\epsilon$ , which is a component of the shear part and thus it is contaminated by shear.

## 1.2.6 Liutex

### 1.2.6.1 Definition of Liutex

Liutex is defined as the rigid rotation part of fluid motion [4–6]. The mathematical definition of Liutex is presented by Eq. 1.8 [32]:

$$\vec{R} = R \vec{r} \quad (1.8a)$$

$$R = (\vec{\omega} \cdot \vec{r}) - \sqrt{(\vec{\omega} \cdot \vec{r})^2 - 4\lambda_{ci}^2}, \quad \vec{\omega} \cdot \vec{r} > 0 \quad (1.8b)$$

where  $\vec{R}$  and  $R$  are Liutex vector and magnitude,  $\vec{r}$  is the real eigenvector of  $\nabla \vec{v}$ ,  $\vec{\omega} = \nabla \times \vec{v}$  is vorticity, and  $\lambda_{ci}$  is the imaginary part of the conjugate complex eigenvalues of  $\nabla \vec{v}$ . The condition  $\vec{\omega} \cdot \vec{r} > 0$  is used to keep the definition unique and consistent when the fluid motion is pure rotation.

### 1.2.6.2 Vorticity Versus Vortex

The major mathematical misunderstanding of the first generation of vortex identification methods is the consideration of vorticity vector as the fluid rotation axis and vorticity magnitude as the vortex strength (angular speed). In the following, it is shown that *vorticity is not the fluid rotation axis*.

**Definition 1.1** At a moment, a local fluid rotation axis is defined as a vector that can only have stretching (compression) along its length.

It is basic math that the increment of  $\vec{v}$  in the direction of  $d\vec{r}$  is  $d\vec{v} = \nabla \vec{v} \cdot d\vec{r}$ .

**Theorem 1.1** Liutex is the local fluid rotation axis.

**Proof** In the Liutex direction, which is the real eigenvector,  $d\vec{v} = \nabla \vec{v} \cdot \vec{r} = \lambda_r \vec{r}$ .

According to Definition 1.1, Liutex is the local rotation axis as  $\vec{R} = R \vec{r}$ .

**Theorem 1.2** Vorticity is, in general, **not** the local fluid rotation axis.

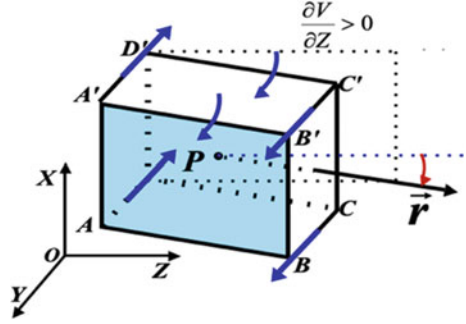
**Proof**

$$\begin{aligned} d\vec{v} &= \nabla \vec{v} \cdot \vec{\omega} = \mathbf{A} \cdot \vec{\omega} + \mathbf{B} \cdot \vec{\omega} = \mathbf{A} \cdot (a_1 \vec{r}_1 + a_2 \vec{r}_2 + a_3 \vec{r}_3) + (\nabla \times \vec{v}) \times \vec{\omega} \\ &= a_1 \lambda_1 \vec{r}_1 + a_2 \lambda_2 \vec{r}_2 + a_3 \lambda_3 \vec{r}_3 + 0 \neq \lambda (a_1 \vec{r}_1 + a_2 \vec{r}_2 + a_3 \vec{r}_3) = \lambda \vec{\omega} \quad (1.9) \end{aligned}$$

Unless  $\lambda_1 = \lambda_2 = \lambda_3 = \lambda$  or for rigid rotation where  $\lambda_1 = \lambda_2 = 0$ .



**Fig. 1.3** Principal coordinates



### 1.2.6.3 Principal Coordinate and Principal Decomposition

**Principal Coordinate.** In the vortex area, the velocity gradient tensor must have one real eigenvalue and two conjugate complex eigenvalues [44]. In Fig. 1.3, the Z-axis of a principal coordinate (X, Y, Z) is aligned with the real eigenvector of  $\nabla \vec{v}$  and two diagonal elements that are equal to each other. In the principal coordinate:

$$\nabla \vec{V} = \begin{bmatrix} \frac{\partial U}{\partial X} & \frac{\partial U}{\partial Y} & 0 \\ \frac{\partial V}{\partial X} & \frac{\partial V}{\partial Y} & 0 \\ \frac{\partial W}{\partial X} & \frac{\partial W}{\partial Y} & \frac{\partial W}{\partial Z} \end{bmatrix} = \begin{bmatrix} \frac{\partial U}{\partial X} & \frac{\partial U}{\partial Y} & 0 \\ \frac{\partial V}{\partial X} & \frac{\partial V}{\partial Y} & 0 \\ \frac{\partial W}{\partial X} & \frac{\partial W}{\partial Y} & \lambda_r \end{bmatrix} \quad (1.10)$$

$$\nabla \vec{V}_\theta = \begin{bmatrix} \lambda_{cr} & -\frac{1}{2}R & 0 \\ \frac{1}{2}R + \epsilon & \lambda_{cr} & 0 \\ \xi & \eta & \lambda_r \end{bmatrix} \quad (1.11)$$

where  $R$  is the Liutex magnitude,  $\lambda_r$  is the real eigenvalue,  $\lambda_{cr}$  is the real part of the conjugated complex eigenvalues, and  $\xi, \eta, \epsilon$  are shears.

### 1.2.6.4 UTA R-NR Principal Tensor Decomposition

The first author Dr. Liu has proposed a new Liutex-based tensor decomposition, i.e., *UTA R-NR tensor*, to replace the traditional Cauchy-Stokes (Helmholtz) decomposition. The *UTA R-NR* velocity gradient tensor decomposition can be written as:

$$\nabla \vec{V} = \mathbf{R} + \mathbf{NR} \quad (1.12)$$

where

$$\mathbf{R} = \begin{bmatrix} 0 & -R/2 & 0 \\ R/2 & 0 & 0 \\ 0 & 0 & 0 \end{bmatrix} \quad (1.13)$$

and

$$\mathbf{NR} = \begin{bmatrix} \lambda_{cr} & 0 & 0 \\ \epsilon & \lambda_{cr} & 0 \\ \xi & \eta & \lambda_r \end{bmatrix} \quad (1.14)$$

therefore,

$$\nabla \vec{\mathbf{V}} = \begin{bmatrix} \lambda_{cr} & -R/2 & 0 \\ R/2 + \epsilon & \lambda_{cr} & 0 \\ \xi & \eta & \lambda_r \end{bmatrix} \quad (1.15)$$

where  $\mathbf{R}$  stands for the rotational part of the local fluid motion, which is the tensor version of Liutex, and  $\mathbf{NR}$  is the non-rotational part. It is clear that  $\mathbf{NR}$  has three real eigenvalues, so  $\mathbf{NR}$  itself implies no local rotation. The *UTA R-NR decomposition is important to vortical flow and turbulent flow.*

### 1.2.6.5 Vorticity RS Decomposition

Vorticity cannot be applied to represent flow rotation; otherwise, we would not need vortex identification methods like  $Q$ ,  $\lambda_{ci}$ ,  $\lambda_2$ ,  $\Delta$ . The vorticity vector must be decomposed to a rotational part (Liutex) and a non-rotational part (shear). The vorticity RS decomposition can be obtained from Eq. 1.16.

$$\vec{\omega} = \nabla \times \vec{\mathbf{V}} = \vec{\mathbf{R}} + \vec{\mathbf{S}} = \begin{bmatrix} 0 \\ 0 \\ R \end{bmatrix} + \begin{bmatrix} \eta \\ -\xi \\ \epsilon \end{bmatrix} \quad (1.16)$$

where  $\vec{\mathbf{S}} = \vec{\omega} - \vec{\mathbf{R}}$  can be considered as a shearing vector since the components of  $\vec{\mathbf{S}}$  indicate the strengths of the simple shear along different axes. Note that the vorticity in the vortex legs is almost shear  $\vec{\mathbf{S}}$ , but not rotation  $\vec{\mathbf{R}}$  (Fig. 1.4). Again, vorticity cannot represent vortex.

### 1.2.6.6 Liutex-Based Vortex Identification Methods

**Liutex Iso-surface.** Since Liutex is the rigid rotational part that is extracted from fluid motion, the Liutex vector, Liutex vector lines, Liutex tubes, and Liutex iso-surface

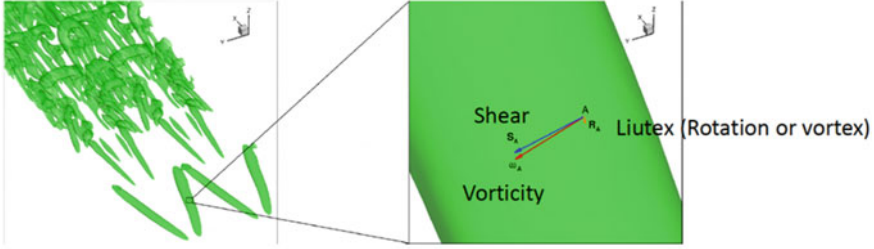


**Fig. 1.4** Illustration of vorticity vector decomposition at Point A

can all be applied to display the vortex structure (Fig. 1.5). The advantage of the Liutex method is that Liutex is a vector, unlike others which are all scalar. Another benefit of Liutex is that it represents pure rotation without contamination by shears, while all other vortex identification methods are contaminated by shears. Of course, the Liutex iso-surface still needs thresholds like other scalar methods, but it is the pure rotation strength.

**Omega Method.** The  $\Omega$  method is given by Eq. 1.17:

$$\Omega = \frac{\|\mathbf{B}\|_F^2}{\|\mathbf{A}\|_F^2 + \|\mathbf{B}\|_F^2 + \varepsilon} \tag{1.17}$$

where  $\mathbf{A}$  and  $\mathbf{B}$  are the symmetric and antisymmetric parts from Cauchy-Stokes decomposition,  $\varepsilon$  is a small positive number introduced to avoid division by zero or extremely small numbers, and  $\|\mathbf{A}\|_F$  is the Frobenius norm  $\varepsilon$  that can be determined at each time step from Eq. 1.18 [19].

$$\varepsilon = 0.001(\|\mathbf{B}\|_F^2 - \|\mathbf{A}\|_F^2)_{max} \tag{1.18}$$

The advantages of the  $\Omega$  method include: (i) it is easily performed, (ii) it has a clear physical meaning, (iii) it is normalized from 0 to 1, (iv) it is insensitive to threshold adjustments by setting  $\Omega=0.52$ , and (v) it can capture both strong and weak vortices simultaneously.

**Modified Liutex-Omega Method.** The modified Liutex-Omega method combines the ideas of both the Liutex and Omega methods, which is normalized, not contaminated, by shear and is insensitive to threshold selection. The modified Liutex-Omega method is defined by Eq. 1.19.

$$\tilde{\Omega}_R = \frac{\beta^2}{\beta^2 + \alpha^2 + \lambda_{cr}^2 + \frac{1}{2}\lambda_r^2 + \varepsilon} \tag{1.19}$$

where

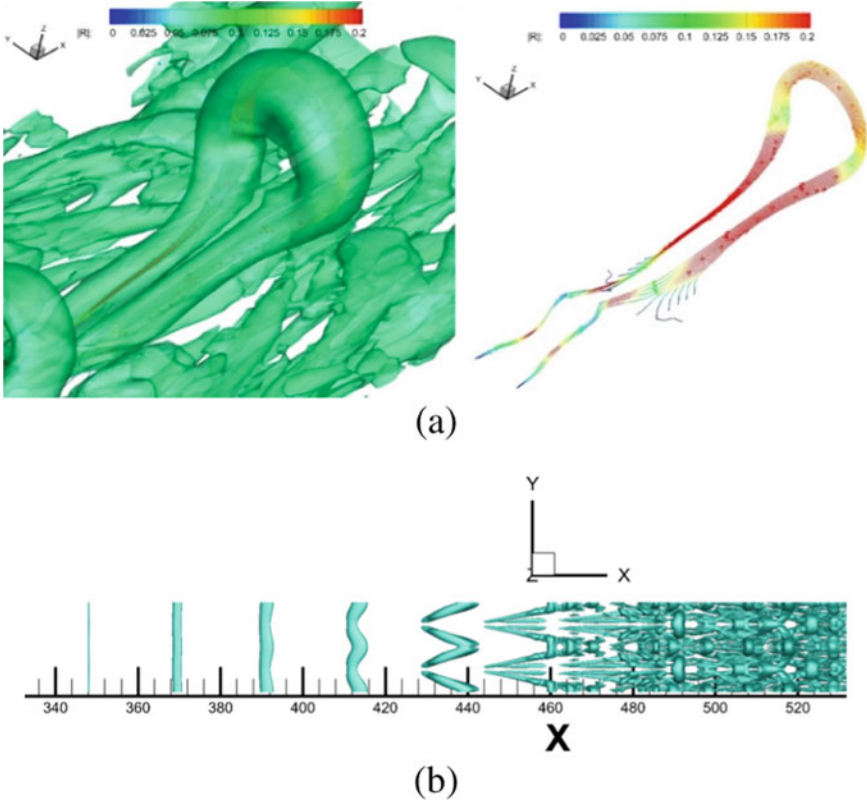


**Fig. 1.5** (a) Liutex iso-surface and Liutex lines (color represents the rotation strength), and (b) Liutex iso-surface for the vortex structure in early transition ( $R = 0.1$ )

$$\alpha = \frac{1}{2} \sqrt{\left(\frac{\partial V}{\partial Y} - \frac{\partial U}{\partial X}\right)^2 + \left(\frac{\partial V}{\partial X} + \frac{\partial U}{\partial Y}\right)^2} \quad (1.20a)$$

$$\beta = \frac{1}{2} \left(\frac{\partial V}{\partial X} - \frac{\partial U}{\partial Y}\right) \quad (1.20b)$$

Equation 1.20 is equivalent to

$$\tilde{\Omega}_R = \frac{(\vec{\omega} \cdot \vec{r})^2}{2\left[(\vec{\omega} \cdot \vec{r})^2 - 2\lambda_{ci}^2 + 2\lambda_{cr}^2 + \lambda_r^2\right] + \varepsilon} \quad (1.21)$$

**Liutex Core Line Method.** All iso-surface methods are threshold-dependent. A Liutex core line is defined as the rotation axis of each vortex and is unique and threshold-free. The vortex core line is defined as a special Liutex line that passes

through the points satisfying the condition expressed by Eq. 1.22.

$$\nabla R \times \vec{r} = 0, \quad \vec{r} \neq 0 \tag{1.22}$$

where  $\vec{r}$  represents the direction of the Liutex vector. The Liutex (vortex) rotation core lines are uniquely defined without any threshold requirement (Fig. 1.6). Therefore, the Liutex core rotation axis lines with Liutex strength are derived uniquely and are believed to be the only entity capable of cleanly and unambiguously representing vortex structures. Figure 1.6c shows that it is possible to use the automatic Liutex- core-line method to show the vortex structure; still, we have a long way to go from improving the method enough that it shows the vortex structure uniquely and automatically for turbulence. Figure 1.7 provides a comparison of  $Q$ -criteria and Liutex-core-line methods and indicates that the  $Q$ -criteria is threshold-dependent and unable to capture weak vortices, in contrast to the Liutex-core-line method, which is threshold-free and able to capture both strong and weak vortices.

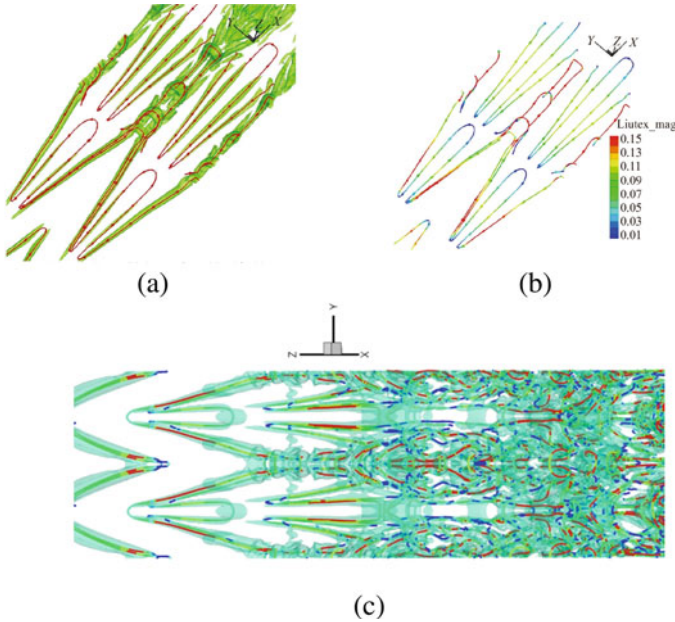


**Fig. 1.6** Vortex structure in flow transition displayed by Liutex core line methods (color represents Liutex strength): (a) Liutex iso-surface and core lines, (b) Liutex core lines, c Liutex core lines for flow transition (preliminary results)

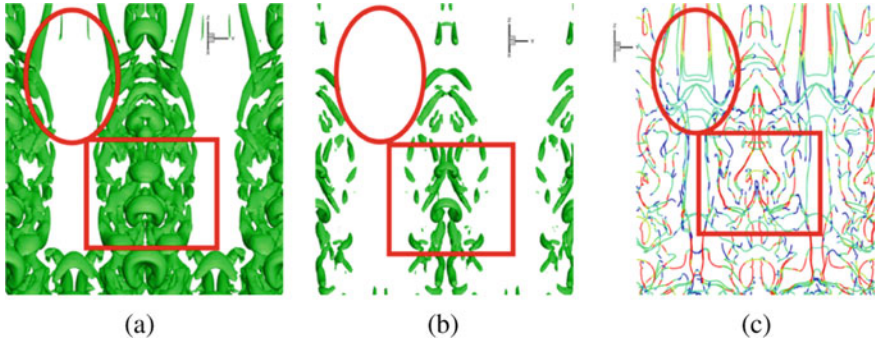


**Fig. 1.7** Comparison of  $Q$ -criteria and Liutex-core-line methods (a)  $Q = 0.005$ , (b)  $Q = 0.05$ , c Liutex-core-line

### 1.3 Future Research Plan

Future research on Liutex and Litex-based vortex identification methods is inevitable. The following are expected to be achieved through the future research:

- (a) a transformational improvement in the knowledge of fluid kinematics and fluid dynamics through a combination of mathematical approaches, computational simulations, and experimental studies, and uncover and quantify the true nature of vortex and its mathematical definition;
- (b) new vortex identification methods that provide an accurate and unique vortical structure of turbulence;
- (c) quantification of the evolution of vortex geometries and topologies; and
- (d) determination of how the new definition of vortex can be used to quantify turbulent flows and vortex dynamics.

The future research may include the following areas.

#### 1.3.1 *Develop Unique, Accurate, and Threshold-Free Vortex Identification Methods*

Vortex identification methods that are accurate and threshold-free need to be developed. Liutex is a mathematical definition for fluid rotation or vortex, but the iso-surface of Liutex is still threshold-dependent for vortex identification. The modified Liutex-Omega method is insensitive to threshold change and a nice tool for vortex identification; however, it has a small adjustable number of  $\varepsilon$  and thus is still not unique, as a threshold is still needed. The Liutex core line and tube method is the only one that provides a unique vortex structure by defining a special Liutex line that satisfies  $\nabla R \times \vec{r} = 0$ ,  $\vec{r} \neq 0$ . However, Liutex core lines and tubes are currently

located by manual methods, which is not realistic for sophisticated vortex structures in turbulent flow. Several efforts have been made, but the outcome is not yet satisfactory. The key issue is how to find the local maxima of Liutex in a 3-D flow field. The Liutex core line should pass the local Liutex maxima. For 1-D problems, the local maxima should have a first-order derivative of zero and second derivative negative. For 2-D and 3-D problems, the local maxima should have a gradient of Liutex equal to zero and the Hessian matrix, which has all negative eigenvalues.

### 1.3.2 Characterize Vortex Structure

The vortex structure can be studied using experimental modeling and numerical simulations to characterize the vortex structure in flow transition and turbulent flows. The mechanism of flow transition and turbulence generation and sustenance should be explored using experimental and numerical techniques.

Vortex structure is still a mystery. Even very simple questions, e.g., whether hairpin vortices exist in turbulent flows, remain unanswered. In fact, not all researchers believe that hairpin packets exist in turbulent flow. In recent studies, large numbers of hairpin packets were observed in low Reynolds number flows [44], but no hairpin vortices were observed at high Reynolds numbers [45, 46]. This disagreement exists since there is no rigorous mathematical vortex definition. Additionally, the iso-surface of existing vortex identification methods are all threshold-dependent but not unique. The new vortex identification may be used to find unique vortex structures. Flow visualization can provide hints on how large vortices are generated and how they become non-symmetric and chaotic. A qualitative comparison between the results from PIV and DNS and statistical analysis of flow field can be used to extract vortex characteristics at the range of  $Re_\delta = 500\text{--}4000$ . This range of friction Reynolds number covers transitional flows and low-to-high Reynolds number turbulent flows. The vortex structure and its temporal and spatial evolution can be studied by conducting experiments to capture the hairpin structure, multi-layer vortices, and vortex merging.

### 1.3.3 Liutex Similarity

The energy transformation paths between the large and small vortices will be investigated by DNS and experiments. The most successful theory of turbulence is the *second Kolmogorov similarity K41* [47] in the inertial subrange ( $l_{EI} > l > l_{DI}$ ). According to K41, the energy spectrum  $E_k(f)$  of turbulence must be of the form of Eq. 1.23, which is the famous  $-5/3$  law.

$$E_k(f) = C \varepsilon_0^{\frac{2}{3}} f^{-\frac{5}{3}} \quad (1.23)$$

where  $f$  is the wavenumber and  $\varepsilon_0$  is the turbulence energy dissipation. The similarity is based on Kolmogorov's third hypothesis, which assumes that in the inertial subrange, the turbulence energy spectrum is solely determined by energy dissipation and the wave number, independent of viscosity. This will give  $E_k(f) = C\varepsilon_0^a f^b$ , where the dimension of wave number  $f$  is  $1/m$ . The power coefficients  $a$  and  $b$  are easily obtained by dimensional analysis; however, Kolmogorov's law requires homogeneous incompressible flow with a very high Reynolds number and is for the inertial subrange. It is hard to match DNS data and experimental results in a turbulent boundary layer.

There is no similarity for vorticity and  $Q$ -criterion (Fig. 1.8a, b); however, the Liutex similarity [36] is found in a low Reynolds number turbulent boundary layer in the subrange of dissipation (Fig. 1.8c), which is important for a subgrid model in LES. The Liutex similarity, which has been reported by a number of authors, cannot be an accident because it is very meaningful for finding turbulence structure and turbulence sub-grid modeling. However, it is still unknown why the Liutex spectrum meets the  $-5/3$  law and how the Liutex  $-5/3$  law can be used for turbulence modeling. The exact Liutex similarity provides a powerful tool for studying turbulence structure and developing a reliable subgrid model of large eddy simulation, which is one of the goals of this research. Similarity is the foundation for subgrid modeling.

### ***1.3.4 Correlation Analysis of Pressure Fluctuation (Noise Generation) and Liutex Spectrum by Mathematical Analysis and Experimental Modeling***

A high-order large eddy simulation (LES) of a micro vortex generator (MVG) is conducted to control the flow separation induced by shock and the turbulent boundary layer interaction (SBLI) at Mach number 2.4 in a compression corner. A low frequency of pressure oscillation caused by SBLI has been one of the major hurdles of supersonic commercial aircraft design for decades. Liutex is a kinematic definition that works for both incompressible and compressible flow. We found that pressure oscillation and the Liutex spectrum are closely correlated, over 0.9 at most points (Fig. 1.9 and Table 1.1), which could help in finding the mechanism of the low-frequency noise generation and learning how to reduce or remove the noise. It cannot be an accident that the correlation is high for the turbulent boundary layer, as shown in a recent study. As the pressure fluctuation is found closely correlated with the Liutex spectrum, it is hoped that a new theory can be developed on shock waves and turbulent boundary layer interactions that will lead to new technology for controlling SBLI, which is the bottleneck of commercial aircraft design. The theory and control of SBLI require additional research.

A new technique for controlling the supersonic boundary layer flow is to distribute an array of MVGs, whose height is less than the boundary layer thickness, ahead of the region with adverse flow conditions. In contrast to the conventional vortex



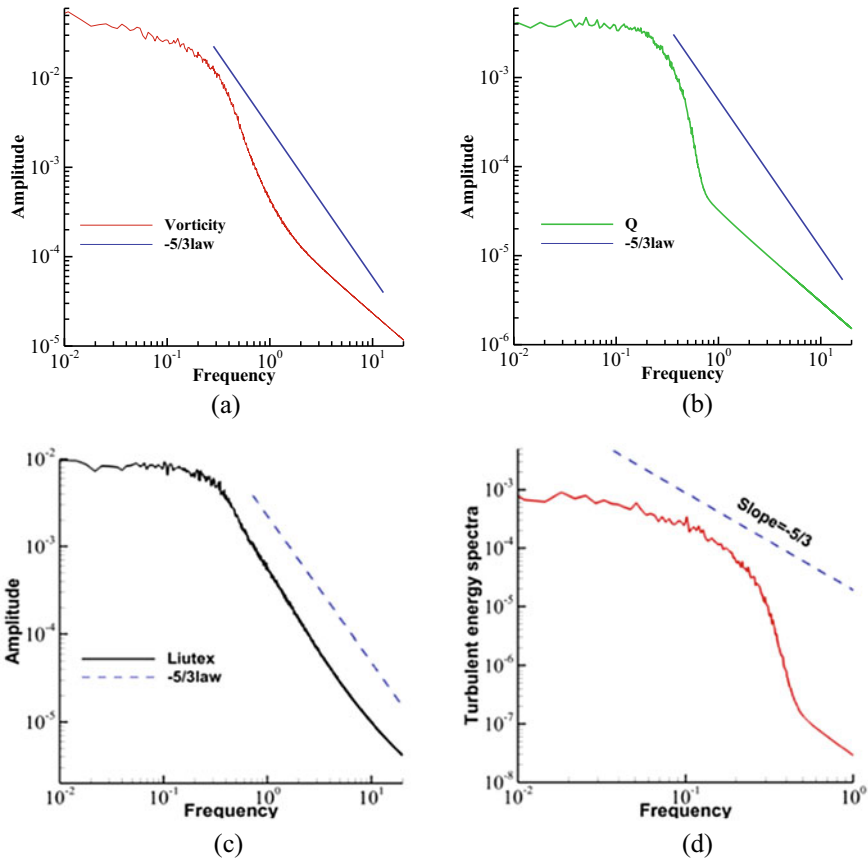


**Fig. 1.8** Energy spectrum: (a) vorticity, (b)  $Q$ -criterion, (c) Liutex  $-5/3$  similarity and (d) Kolmogorov K41 similarity

generator with a height comparable to the boundary layer thickness, an MVG’s height is about 20–60% of the boundary layer thickness.

An MVG appears to reduce the size of the separation zone. It has been suggested that the boundary layer is energized by the MVGs from a system of streamwise counter-rotating vortices. Such a mechanism has recently been studied in detail in low-speed experiments. A series of ring-like vortices (Fig. 1.8b) generated behind MVG was discovered by our previous LES, and the numerical discoveries of the ring-like vortex structure were confirmed by the 3-D PIV experiment. A V-shaped separation zone was discovered on the wall boundary by the LES. The length of the separation at the two spanwise sides of the domain was estimated to be around 6–6.5 h (height of the MVG), and the length at the centerline was estimated to be around 5 h in supersonic flow with  $Ma = 2.5$ . Compared with the value of 8.2–8.4 h for the ramp-only case, the MVG significantly reduces the separation region. It was also confirmed that the interaction between ring-like vortices and a ramp shock wave is the mechanism for forming the V-shaped separation zone and the flow

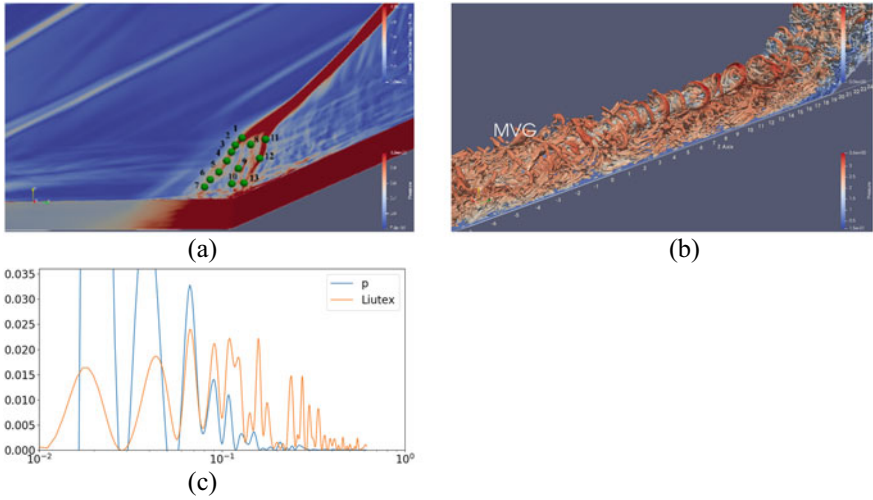


**Fig. 1.9** Correlation of spectrum of pressure fluctuation and Liutex: (a) 13 sample points, (b) shock boundary layer interaction, (c) spectrum of pressure, and Liutex at Point 5

**Table 1.1** Correlation Coefficient ( $r$ ) of the Spectra at the First Seven Points in Fig. 1.9a

Point #	1	2	3	4	5	6	7
$r$	88.4%	86.3%	93.7%	95.5%	94.6%	97.0%	91.4%

separation reduction at the ramp corner. The vortex structure in MVG needs to be examined through numerical simulations and be compared the results with those from experiments.

### 1.4 Conclusions and Future Work

Based on abovementioned understanding, following conclusions can be made:

1. As the first generation of vortex identification, vorticity is a vector, but cannot be used to represent vortex. Vorticity is curl of velocity, but vortex is fluid rotation. They are two different vectors.
2. As the second generation of vortex identification criteria,  $Q$ ,  $\Delta$ ,  $\lambda_2$ , and  $\lambda_{ci}$  methods are all scalars and thus strongly dependent on the arbitrary thresholds. They cannot show the vortex rotation axis, and are all contaminated by stretching (compression) and shearing.
3. Liutex is the third generation of vortex definition and identification, which is the only quantified and mathematical definition of local fluid rotation or vortex vector.

4. Liutex can give right direction and strength for group fluid rotation or natural vortices. In other words, vortex core is a special Liutex vector, Liutex tube, and concentration of Liutex lines.
5. Liutex vector, line, tube, core lines can all be correctly applied for vortex structure, but vortex structure cannot be visualized by the first and second generations since they are threshold-dependent, not unique, and shear-contaminated.
6. Modified Liutex-Omega method is insensitive to threshold change.
7. Liutex-core-line method is unique, threshold-free, accurate to visualize vortex structure including direction and strength.

Future research should integrate mathematical analysis, direct measurements, and numerical simulations to advance the knowledge and understanding of vortex structure and evolution. These advancements will improve vortex identification and quantification methods. The new vortex identification methods are accurate, unique, and threshold-free and will be used to formulate Liutex dynamics for quantified research on vortex and turbulence. The Liutex similarity will provide a powerful tool for studying turbulence structure and developing a reliable sub-grid model of LES. The results from future research will lead to quantified research of turbulence generation and sustenance and pave the way for developing new governing equations using Liutex, which may enhance turbulence calculations and modeling. These outcomes will significantly impact basic mathematics and fundamental fluid mechanics by introducing a new definition of vortex into turbulence research. New fluid kinematics can be established using the Liutex theoretical system to replace existing fluid kinematics and possibly launch new turbulence dynamics.

**Acknowledgements** The first author is grateful to the University of Texas at Arlington (UTA) for long-time support as a tenured faculty member. The authors also thank Texas Advanced Computing Center (TACC) for long-term support in the provision of computation hours.

**Data Availability** The data supporting this study's findings are available from the corresponding author upon reasonable request.

## References

1. D. Küchemann, Report on the IUTAM symposium on concentrated vortex motions in fluids. *J. Fluid Mech.* **21**, 1–20 (1965)
2. H. Helmholtz, Über Integrale der hydrodynamischen Gleichungen, welche den Wirbelbewegungen entsprechen. *Journal für die reine und angewandte Mathematik* **55**, 25–55 (1858)
3. S. Robinson, S. Kline, P. Spalart, A review of quasi-coherent structures in a numerically simulated turbulent boundary layer. Tech. rep., NASA TM-102191(1989)
4. C. Liu, Y. Gao, S. Tian, X. Dong, Rortex—A new vortex vector definition and vorticity tensor and vector decompositions. *Phys. Fluids* **30**, 035103 (2018). <https://doi.org/10.1063/1.5023001>
5. Y. Gao, C. Liu, Rortex and comparison with eigenvalue-based vortex identification criteria. *Phys. Fluids* **30**, 085107 (2018). <https://doi.org/10.1063/1.5040112>

6. C. Liu, Y. Gao, X. Dong, J. Liu, Y. Zhang, X. Cai, N. Gui, Third generation of vortex identification methods: omega and Liutex/Rortex based systems. *J. Hydrodyn.* **31**(2), 1–19 (2019). <https://doi.org/10.1007/s42241-019-0022-4>
7. J. Hunt, A. Wray, P. Moin, Eddies, streams, and convergence zones in turbulent flows. Center for turbulence research proceedings of the summer program, 193 (1988)
8. M. Chong, A. Perry, B. Cantwell, A general classification of three-dimensional flow fields. *Phys. Fluids A* **2**, 765–777 (1990)
9. J. Jeong, F. Hussain, On the identification of a vortices. *J. Fluid Mech.* **285**, 69–94 (1995)
10. J. Zhou, R. Adrian, S. Balachandar, T. Kendall, Mechanisms for generating coherent packets of hairpin vortices in channel flow. *J. Fluid Mech.* **387**, 353–396 (1999)
11. P. Chakraborty, S. Balachandar, R.J. Adrian, On the relationships between local vortex identification schemes. *J. Fluid Mech.* **535**, 189–214 (2005)
12. V. Kolář, J. Šístek, Consequences of the close relation between Rortex and swirling strength. *Phys. Fluids* **32**, 091702 (2020). <https://doi.org/10.1063/5.0023732>
13. V. Kolář, Vortex identification: new requirements and limitations. *Int. J. Heat Fluid Flow* **28**(4), 638–652 (2007)
14. Z. Li, Zhang, X., He, F., Evaluation of vortex criteria by virtue of the quadruple decomposition of velocity gradient tensor. *Acta Physics Sinica*, **63**(5), 054704 (2014), in Chinese
15. C. Liu, Y. Wang, Y. Yang, Z. Duan, New Omega vortex identification method. *Sci. China Phys. Mech. Astron.* **59**, 684711 (2016)
16. Y. Gao, J. Liu, Y. Yu, C. Liu\*, A Liutex based definition and identification of vortex core center lines. *J. Hydrodyn.* **31**(2), 774–781 (2019a)
17. Y. Gao, Y. Yu, J. Liu, C. Liu\*, Explicit expressions for Rortex tensor and velocity gradient tensor decomposition. *Phys. Fluids* **31**, 081704 (2019b)
18. Y. Gao, C. Liu\*, Rortex based velocity gradient tensor decomposition. *Phys. Fluids* **31**(1), 011704 (2019c)
19. X. Dong, Y. Wang, X. Chen, Y. Zhang, C. Liu, Determination of epsilon for Omega vortex identification method. *J. Hydrodyn.* **30**(4), 541–548 (2018)
20. X. Dong, Y. Yan, Y. Yang, G. Dong and C. Liu\*, Spectrum study on unsteadiness of shock wave -vortex ring interaction. *Phys. Fluids* **30**, 056101 (2018). <https://doi.org/10.1063/1.5027299>, with (2018b)
21. X. Dong, S. Tian, C. Liu\*, Correlation analysis on volume vorticity and vortex in late boundary layer transition. *Phys. Fluids* **30**, 014105 (2018c)
22. X. Dong, G. Dong, C. Liu\*, Study on vorticity structures in late flow transition. *Phys. Fluids* **30**, 104108 (2018d)
23. X. Dong, Y. Gao, C. Liu\*, New normalized Rortex/vortex identification method. *Phys. Fluids* **31**, 011701 (2019). <https://doi.org/10.1063/1.5066016>
24. X. Dong, X. Cai, Y. Dong, C. Liu\*, POD analysis on vortical structures in MVG wake by Liutex core line identification. *J. Hydrodyn.* **32**, 497–509 (2020)
25. J. Liu, Y. Gao, C. Liu\*, An objective version of the Rortex vector for vortex identification. *Phys. Fluids* **31**(6), 065112 (2019a). <https://doi.org/10.1063/1.5095624>
26. J. Liu, C. Liu\*, Modified normalized Rortex/vortex identification method. *Phys. Fluids* **31**(6), 061704 (2019b). <https://doi.org/10.1063/1.5109437>
27. J. Liu, Y. Gao, Y. Wang, C. Liu\*, Galilean invariance of Omega vortex identification method. *J. Hydrodyn.* (2019c). <https://doi.org/10.1007/s42241-019-0024-2>
28. J. Liu, Y. Gao, Y. Wang, C. Liu\*, Objective Omega vortex identification method. *J. Hydrodyn.* (2019d). <https://doi.org/10.1007/s42241-019-0028-y>
29. J. Liu, Y. Deng, Y. Gao, S. Charkrit, C. Liu\*, Mathematical foundation of turbulence generation from symmetric to asymmetric Liutex. *J. Hydrodyn.* **31**(3), 632–636 (2019e)
30. Y. Wang, Y. Yang, G. Yang, C. Liu\*, DNS study on vortex and vorticity in late boundary layer transition. *Comm. Comp. Phys.* **22**, 441–459 (2017)
31. Y. Wang, Y. Gao, C. Liu\*, Galilean invariance of Rortex. *Phys. Fluids* **30**, 111701 (2018). <https://doi.org/10.1063/1.5058939>

32. Y. Wang, Y. Gao, J. Liu, C. Liu\*, Explicit formula for the Liutex vector and physical meaning of vorticity based on the Liutex-Shear decomposition. *J. Hydrodyn.* (2019a). <https://doi.org/10.1007/s42241-019-0032-2>
33. Y. Wang, Y. Gao, C. Liu\*, Letter: Galilean invariance of Rortex. *Phys. Fluids* **30**(11), 111701 (2019b)
34. Y. Wang, Y. Gao, H. Xu, X. Dong, J. Liu, W. Xu, M. Chen, C. Liu\*, Liutex theoretical system and six core elements of vortex identification. *J. Hydrodyn.* **32**, 197–221 (2020)
35. W. Xu, Y. Gao, Y. Deng, J. Liu, C. Liu\*, An explicit expression for the calculation of the Rortex vector. *Phys. Fluids* **31**, 095102 (2019a). <https://doi.org/10.1063/1.5116374>
36. W. Xu, Y. Wang, Y. Gao, J. Liu, H. Dou, C. Liu\*, Liutex similarity in turbulent boundary layer. *J. Hydrodyn.* **31**(6), 1259–1262 (2019b)
37. H. Xu, X. Cai, C. Liu\*, Liutex core definition and automatic identification for turbulence structures. *J. Hydrodyn.* **31**(5), 857–863 (2019)
38. Y. Zhang, X. Qiu, F. Chen, K. Liu, Y. Zhang, X. Dong, C. Liu\*, A selected review of vortex identification methods with applications. *J. Hydrodyn.* **30**(5) (2018). <https://doi.org/10.1007/s42241-018-0112-8>
39. Y. Zhang, X. Wang, Y. Zhang, C. Liu, Comparisons and analyses of vortex identification between Omega method and Q criterion. *J. Hydrodyn.* **31**(2), 224–230 (2019)
40. C. Liu, H. Xu, X. Cai, Y. Gao, *Liutex and Its Applications in Turbulence Research*, ISBN-13: 978–0128190234, ISBN-10: 012819023X, Elsevier, Oct 2020a
41. C. Liu, Y. Gao, *Liutex-based and Other Mathematical, Computational and Experimental Methods for Turbulence Structure*, Vol. 2, ISSN: 2589–2711, eISSN: 2589–272X (Online), ISBN: 978–981–14–3758–8, eISBN: 978–981–14–3760–1 (Online), Bethman, April 2020b
42. C. Truesdell. *The Kinematics of Vorticity*. (Indiana University Publications Science Seres Nr. 14.) XVII + 232 S. Bloomington (1954). Indiana University Press
43. S. Robinson, A review of vortex structures and associated coherent motions in turbulent boundary layers, in *Structure of Turbulence and Drag Reduction*, Springer, Berlin, Heidelberg (1990)
44. X. Wu, P. Moin, Direct numerical simulation of turbulence in a nominally zero-pressure gradient flat-plate boundary layer. *J. Fluid Mech.* **630**, 5–41 (2009)
45. I. Marusic, B.J. McKeon, P.A. Monkewitz, H.M. Nagib, A.J. Smits, K.R. Sreenivasan, Wall-bounded turbulent flows at high Reynolds numbers: recent advances and key issues. *Phys. Fluids* **22**, 065103 (2010)
46. J. Jiménez, Coherent structures in wall-bounded turbulence. *J. Fluid Mech.* **842**, P1 (2018). <https://doi.org/10.1017/jfm.2018.144>
47. AN. Kolmogorov Local structure of turbulence in an incompressible fluid at very high Reynolds numbers. *Dokl. Akad. Nauk. SSSR* **26**: 115–18 (1941)